sustainability

MDPI

Article

Optimizing Sustainable Phytoextraction of Lead from Contaminated Soil Using Response Surface Methodology (RSM) and Artificial Neural Network (ANN)

Maria Manzoor [1,2,*], Usman Rauf Kamboh [3,4], Sumaira Gulshan [4], Sven Tomforde [3,*], Iram Gul [5], Alighazi Siddiqui [6] and Muhammad Arshad [1]

1 Institute of Environmental Sciences and Engineering, School of Civil and Environmental Engineering, National University of Sciences and Technology, Islamabad 44000, Pakistan; marshad@iese.nust.edu.pk
2 Institute of Plant Nutrition and Soil Science, Christian-Albrechts-Universität, 24118 Kiel, Germany
3 The Intelligent System Group, Christian-Albrechts-Universität, 24118 Kiel, Germany; usmanrouf87@gmail.com
4 Department of Computational Sciences, The University of Faisalabad, Faisalabad 38000, Pakistan; simi66183@gmail.com
5 Department of Earth and Environmental Sciences, Hazara University, Mansehra 21300, Pakistan; iram.k87@gmail.com
6 Department of Computer Science, College of Computer Science & Information Technology, Jazan University, Jazan 45152, Saudi Arabia; aanwar@jazanu.edu.sa
* Correspondence: mmanzoor@plantnutrition.uni-kiel.de (M.M.); st@informatik.uni-kiel.de (S.T.); Tel.: +49-431-880-4844 (M.M.)

Abstract: Lead (Pb) is well known for the containment of soil surfaces. In the last few decades, phytoremediation has been the most ideal technology to extract Pb from soil, involving numerous chemical reactions and cost analysis. The aim of this study is to model and to optimize Pb extraction from the contaminated soil via *Pelargonium hortorum* by comparing two modeling approaches: response surface methodology (RSM) and artificial neural networks (ANNs) with the genetic algorithm (GA). To determine the significance of the proposed solution, *in vitro* essays were performed to check the Pb tolerance of bacterial strains (NCCP 1844, 1848, 1857, and 1862), followed by the co-application of bacteria and citric acid on a Pb hyperaccumulator (*Pelargonium hortorum* L.) on Murashige and Skoog (MS) agar medium. Afterwards, a pot culture experiment was performed to optimize Pb extraction competency from Pb-spiked (0 mg kg^{-1}, 500 mg kg^{-1}, 1000 mg kg^{-1}, and 1500 mg kg^{-1}) soil by *Pelargonium hortorum* L., to which citric acid (5 and 10 mmol L^{-1}) and *Microbacterium paraoxydance* (1 and 1.5 OD) were applied. Plants were harvested at 30, 60, and 90 day intervals, and they were analyzed for dry biomass and Pb uptake characteristics. The maximum Pb extraction efficiency of 86.0% was achieved with 500 mg kg^{-1} soil Pb for 60 days. Furthermore, RSM, based on the Box–Behnken design (BBD) and the ANN-based Levenberg–Marquardt Algorithm (LMA), were applied to model Pb extraction from the soil. The significance of the predicted values from RSM and LMA were close to 36.0% and 86.05%, respectively, compared to the laboratory values. The comprehensive evaluation of these findings encouraged the accuracy, reliability, and efficiency of the ANN for the optimization process. Therefore, experimental results showed that ANN is an accurate technique to optimize an integrated phytoremediation system for sustainable Pb removal, besides being environmentally friendly and potentially cost-effective.

Keywords: soil contamination; citric acid; bacteria; ANN; RSM

check for updates

Citation: Manzoor, M.; Kamboh, U.R.; Gulshan, S.; Tomforde, S.; Gul, I.; Siddiqui, A.; Arshad, M. Optimizing Sustainable Phytoextraction of Lead from Contaminated Soil Using Response Surface Methodology (RSM) and Artificial Neural Network (ANN). *Sustainability* **2023**, *15*, 11049. https://doi.org/10.3390/su151411049

Academic Editor: Andres Seco Meneses

Received: 19 May 2023
Revised: 17 June 2023
Accepted: 3 July 2023
Published: 14 July 2023

1. Introduction

Lead, along with other heavy metals in the soil surface, is found to be immensely important concerning ecohealth. The "Agency for Toxic Substances and Disease Registry" has ranked Pb as the second-most hazardous substance [1], and the US Environmental

Protection Agency also placed Pb on the top priority list. Owing to its carcinogenic nature, non-biodegradability, low mobility, and persistence in soil for years, it becomes a continuous threat to human life [2,3]. Although it is naturally present in soil, ranging from 50 to 500 mg kg^{-1} [4], an increased concentration is directly accumulated owing to anthropogenic activities, including the recycling of lead–acid batteries, fossil fuel burning, leaded paints, and automobile emissions. Lead does not have a biological function in plant growth and development. Rather, its increased concentration causes the dysfunction of important biogeochemical cycles, and this disturbs nutrient mineralization by the toxifying microbial community and enzymatic activities in soil [5]. In plants, lead causes oxidative stress and negatively affects morphological, physiological, and biochemical processes, whereas in humans, Pb has been reported to cause neurological, hematological, reproductive, and kidney disorders [6]. Therefore, the remediation of Pb-contaminated soil is a required priority.

The traditional remediation techniques include different physical and chemical methods. However, unfortunately, most of these methods do not completely extract Pb. Instead, they just transfer it from one medium to another or convert its chemical form [7]. In this context, phytoremediation is currently in the state of research and offers environmentally friendly and green technologies to permanently remove Pb from soil using Pb hyperaccumulator plants, such as *P. hortorum*, *Phyllostachys pubescens*, and *Iris halopilla* [8,9]. To increase phytoremediation efficiency, different plant-growth-promoting (PGP) bacteria, such as *M. paraoxydance*, *Pseudomonas* (sp.), and organic chelates, such as di N-hydroxy ethylene diaminetriacetic acid (HEDTA), ethylene diaminetetraacetic acid (EDTA), ethylenetriaminepentaacetic acid (DTPA), nitrilotriacetate (NTA), citric acid, and ethylene diamine disuccinate (EDDS), have also been applied, along with the use of plants [10–12]. However, to achieve the Sustainable Development Goals (SDGs) 6, 12, and 15, there is still a need to investigate sustainable solutions, which are, e.g., based on artificial intelligence for safe, cost-effective, and time-efficient solutions for the efficient phytoremediation of Pb. Nowadays, many scientific investigations have made use of important prediction and optimization approaches, which are based on statistical, computational, mathematical, and artificial models, such as ANN, RSM, and GA [13–16]. The ANN model can be used to predict the remediation of Pb with GA, and RSM has been implemented for optimizing the removal condition. Moreover, these models are less complicated, they are inexpensive, and they can provide an accurate finding. The specific advantages of this research are as follows:

- RSM, ANN, and GA were applied to model and to optimize the pb extraction from the contaminated soil by the *Pelargonium hortorum*. The comprehensive evaluation of findings encouraged the accuracy, reliability, and efficiency of ANN for the optimization process.
- Another advantage of this trained algorithm (Levenberg–Marquardt) is best-fit against laboratory responses, in addition to being environmentally friendly and potentially cost-effective.
- The comparison indicates that the prediction capabilities of the ANN model are better than the RSM model because the R^2 of ANN is 0.99 and that of RSM is 0.90.

Moreover, these machine learning-based models—ANN and GA—are less complicated, inexpensive, and they can provide accurate findings. The following study has been designed for optimization of the Pb-removing efficiency of *P. hortorum* L. supplemented with citric acid and plant-growth-promoting-bacteria *M. paraoxydans* using ANN models. The prime goal of this study was to optimize the dosage of citric acid and Pb-resistant bacteria to obtain maximum Pb phytoextraction efficiency and to optimize the integrated phytoremediation system for Pb extraction using RSM, ANN and GA models.

2. Materials and Methods

The flow chart of the experimental design is presented in Figure 1. Briefly, the present study was performed in three steps. In the first step, laboratory-based experimental work was performed for the selection of Pb-resistant bacteria, citric acid concentration, and the dose of Pb concentration for *P. hortorum*. In the second step, a pot culture experiment was performed, and selected bacteria as well as citric acid were applied to increase Pb phytoextraction efficiency of *P. hortorum*. In the third step, the experimental data were used, and ANN and GA models were applied to optimize the enhanced operational conditions of the Pb phytoremediation system.

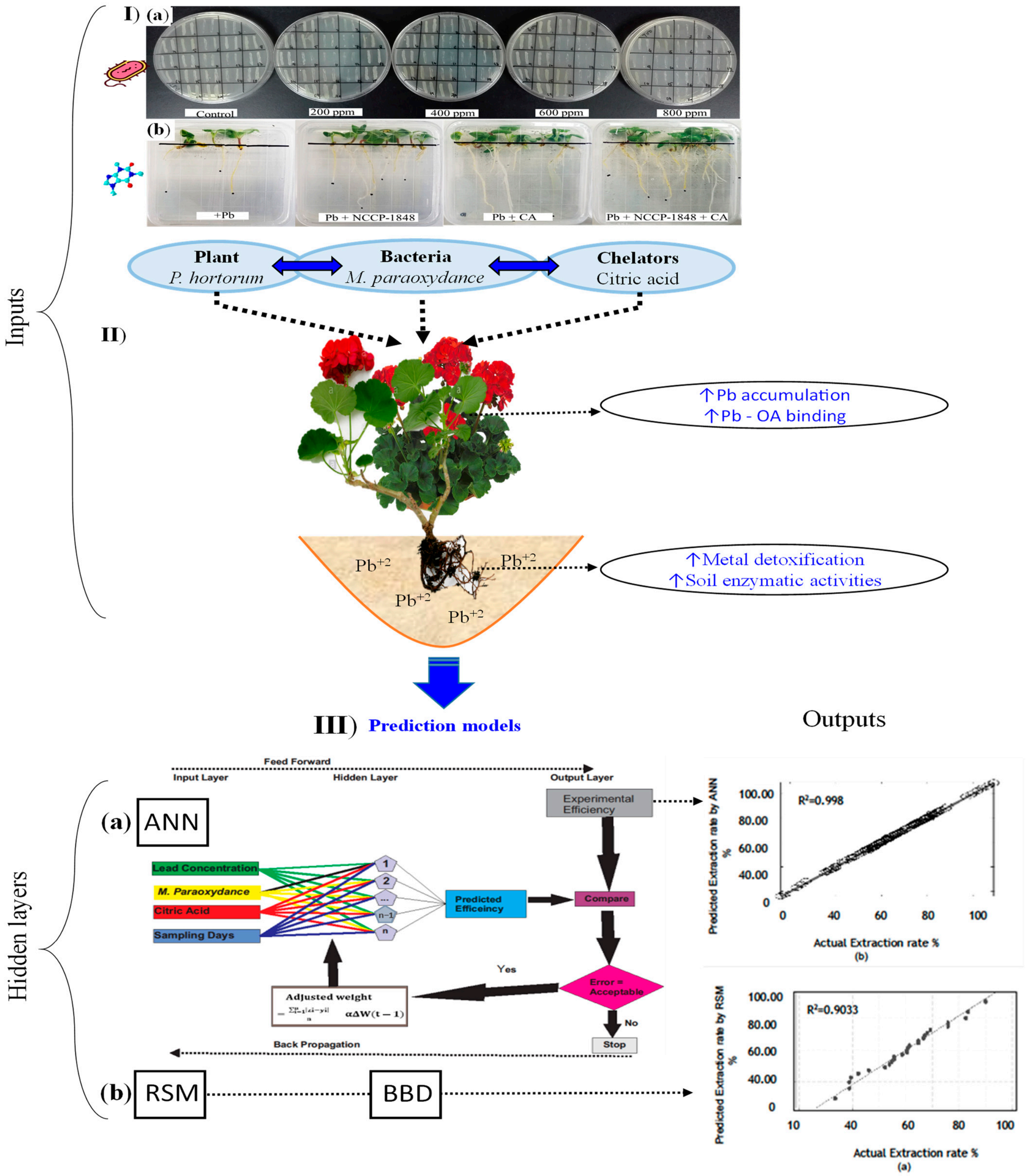

Figure 1. Layout of study. (**I**) Selection of Pb-tolerant bacterial strains on LB agar supplemented with different concentration of Pb (**a**), and effect of *M. paraoxydanse* (1.5 OD) and citric acid (10 mmol L^{-1}) on *P. hortorum* germination under Pb stress (40 mg L^{-1}) (**b**). (**II**) Pot culture experiment with selected doses of bacteria and citric acid. (**III**) Feed-forward back-propagation neural network architecture along with four considered parameters (**a**), and RSM model based on BBD design (**b**), respectively.

2.1. Selection of Pb and Citric Acid Tolerant Bacterial Strains

The growth characteristics of bacterial strains, preisolated by [8], were monitored against a wide range of Pb (0–800 mg L^{-1}) and citric acid (CA) (0–10 mmol L^{-1}) in a Luria–Bertani (LB) medium. The bacteria's ability to tolerate Pb and citric acid was investigated by discovering the minimum inhibition concentrations (MIC) against $C_6H_8O_7$ and $PbCl_2$ on LB agar and broth. Briefly, bacterial strain (200 µL) was inoculated in LB broth medium supplemented with Pb and CA. A shaker incubator was used to incubate the bacteria at 200 rpm and 28 °C. The growth characteristics of strains were investigated by measuring the culture's optical density (OD) at 600 nm after regular intervals (2–36 h) with an ultraviolet–visible spectrophotometer (Specord 200 plus). The tolerance index of bacterial strains against CA and Pb was computed by the division of bacterial dry biomass achieved from the treated group in a controlled environment after 24 h of incubation. Furthermore, the cross-tolerance of CA and Pb to other heavy metals, including zinc (Zn), cobalt (Co), cadmium (Cd), nickel (Ni), and copper (Cu), were also recorded. The bacterial strain that showed the highest tolerance against both Pb and citric acid was found to be *M. paraoxydans* and therefore selected for further studies.

2.2. Germination and Seed Vigor Index (SVI)

The *In vitro* tests were performed at a laboratory scale to monitor the impacts of Pb, citric acid, and *M. Paraoxydans* on seed germination and SVI. Initially, Petri plates of 1/2 Murashige and Skoog (MS) agar medium supplements with different concentrations of Pb (0, 10, 20, 30 & 40 mg L^{-1}) were prepared. For treatments, about 200 µL of bacterial inoculum (1.5 OD) suspension and citric acid solution (10 mmol L^{-1}) were spread on the agar using a glass spreader. The seeds of *P. hortorum* L., obtained from the Awan Garden Center, F7 markaz Islamabad, were disinfected for 30 min soaking in 70% ethanol followed by 30 min in 10% NaClO. The washed seeds (with sterile distilled water) were then incubated on the prepared MS agar Petri plates containing Pb and treatments (citric acid and *M. paraoxydans*). Petri plates were then incubated for 7 days at 25 °C in the dark. After 1 week, the Petri plates were removed from the incubator and monitored for the physiological parameters, such as SVI, germination and seedling root/shoot length, using the following two equations (Equations (1) and (2)) [17–19]:

$$\mathrm{GE}(\%) = \frac{No.\,of\ germinated\ seeds}{Total\ No.\,of\ seeds} \times 10 \tag{1}$$

$$\mathrm{SVI} = \mathrm{L} \times \mathrm{GE} \tag{2}$$

Whereas, GE indicates percentage germinated seeds, and L denotes the mean length.

2.3. Soil Characterization and Preparation

Uncontaminated soil was obtained from the, nursery of National University of Science and Technology, Islamabad, and analyzed for physicochemical characteristics. The characteristics of soil used in the experimental activity are shown in Supplementary Data (see the Supplementary Table S1). It was observed that the experimental soil was clay loam with pH (7.63%) and organic matter (0.83%). For experiment preparations, the air-dried soil was mechanically crushed through a ball mill. The crushed soil was sieved over a 2 mm mesh. The obtained fine soil was spiked with different concentrations of Pb ($PbCl_2$ @ 0 mg kg^{-1}, 500 mg kg^{-1}, 1000 mg kg^{-1} and 1500 mg kg^{-1}). For metal stabilization, the soil was regularly watered (60% moisture content), systematically mixed, and kept for 28 days before use. The Pb concentration in the spiked soils was confirmed by wet digestion, and the concentration of Pb was determined using an atomic absorption spectrophotometer (AAS). It was determined that Pb concentrations were 469, 935, and 1445 mg kg^{-1} in spiked soil of 500, 1000, and 1500 mg kg^{-1} soil Pb treatments, respectively, which indicates a metal recovery of 93.1% [4,5].

2.4. Pot Experimental Setup

To enhance the efficiency of the Pb phytoextraction system, citric acid (Merck Millipore, assay > 99.5%) (@ 0, 5, and 10 mmol L^{-1}) and *M. paraoxydans* (@ 0, 1, and 1.5 OD) were applied individually and in combination to the 4-week-old seedlings of *P. hortorum* L. The duration of the experiment was 4 months, and the sampling was performed after 30, 60, and 90 days to determine the rate of Pb extraction from the soil. Tap water was used to carefully wash the harvested plants. The roots were socked in 0.1 N HCL solutions to remove adsorbed Pb. The plants were then dissected into roots and shoots and were placed in the oven at 65 °C for 3 days for drying. After 5 days, the dry matter was recorded and the plant material was grounded to a fine powder using a grinding mill. The Pb concentration in different plant tissues was examined by following the method of wet digestion [6], and the concentration of total Pb was determined using an AAS.

2.5. Optimizing Pb Removal from Soil Using Prediction Models

2.5.1. Response Surface Methodology

The response surface method (RSM) belongs to the class of the statistical methods and is very efficient from a computational, mathematical and cost-effective point of view. Here, it is used to evaluate the impact of multiple independent variables of chemical processes and the responses of the experiments. For our work, it is sufficient to assess the effects of each and every variable separately or combined with other groups of variables. The approach supports fitting the model, and it is evaluating the problems by using optimizing process parameters. This non-linear multivariate model regulates experimental conditions and the design to achieve the system's best and most reliable response performance, which results in optimal results. Furthermore, it offers a mathematical model that is most compatible with laboratory analytical findings [20]. RSM based on BBD is applied to optimize the experimental conditions.

2.5.2. Box–Behnken Design and Data Analysis

The BBD method was utilized for the optimization of different variables including the solution PH, iconic strength, dispersion solvent and the extraction volume of soil. A two-leveled BBD with four factors was implemented, and the lead removal efficiency of *P. hortorum* L. from the contaminated soil by citric acid and *M. paraoxydans* (Table 1 and Table S2) was used as input. The independent variables with their position values were constructed on their respective outcomes of the initial single-factor tests. Furthermore, Pb removal efficiency is taken as yield (Y) which is the dependent response variable. The independent variables are separately positioned at the coded values as (−1, 0, +1) accordingly. The BBD method contains intercept, squared terms of the product of two factors, and a linear analysis. The correlation among response and independent variables is expressed as a quadratic model (Equation (3) [21]).

$$Y = b_1 + b_2A + b_3B + b_4C + b_5D + b_{13}AB + b_{14}AC + b_{15}AD + b_{23}BC + b_{24}BD + b_{25}CD + b_7A^2 + b_{17}B^2 + b_{27}C^2 \quad (3)$$

Table 1. Ranges of the different independent variables used in the RSM model for evaluation of Pb extraction.

Independent Factor	Units	Symbol	Coded Values		
			−1	**0**	**+1**
Lead concentration	mg kg^{-1}	A	500	1000	1500
M. paraoxydans	OD	B	0	0.75	1.5
Citric acid	mg L^{-1}	C	0	5	10
Sampling days	Days	D	30	60	90
Lead extraction	%				

RSM = Response surface methodology.

In Equation (3), i.e., the lead (Pb) removal from soil, we use this quadratic equation for experiments with random chances of independent values. For the response Y(Pb removal), the four model terms (A, B, C, D) were consequential and indicate the effects of independent parameters (AB, AC, AD, BC, BD, CD) as these are the relationships of the independent variables. A_2, B_2, and C_2 are the effects of independent variables, but b_1 was the model constant. b_1, b_2, b_3 and b_4 were linear coefficients of the model; and b_{13}, b_{14}, b_{15} and b_{23}, b_{24}, and b_{25} as well as b_7, b_{17}, and b_{27} are interaction coefficient values of the linear model. Finally, b_{17} and b_{27} are second-order coefficients for the BBD model.

2.5.3. Artificial Neural Networks Modeling

According to [22,23], an ANN was used to determine the non-linear relations between variables. We used the MATLAB Neural Network Toolbox in version 2020a for modeling the ANN. Here, various variants of neural networks are provided for different applications, but the most frequently used network in the field of environmental sciences is the "Feed-Forward Back Propagation Neural Network" (FFBPNN). In this variant of a neural network, there are multiple inputs that are linked to some outputs. In particular, the network consists of multiple inputs as well as hidden and output layers. Each layer contained a certain number of neurons, in which the number of neurons in the hidden layers is of particular importance for computing the response. The weights assigned to the incoming edges of the neural network are allotted to determine the relationship between layers. The network is trained through training data obtained in laboratory experiments. To attain the suitable response, the error between the actual and predicted response variable is returned to the network as a Loss function for learning purposes, i.e., a feedback-based adaptation of the weights. In Figure 2a, a three-layered neural network is modeled. This network is used to compute the reservoir Pb concentration. After data cleaning, the network is trained through the extraction of laboratory data of 243 numbers through an excel file including four independent variables namely Pb Concentration, *M. paraoxydance*, Citric Acid, days and one dependent variable for Pb extraction. A three-layered neural networks was constructed for computation of Pb Phytoremediation (the use of higher plants for the cost-effective, environmentally rehabilitation of soil by toxic metals) model. Figure 1 shows the ANN model along with the FFBPNN approach. Furthermore, the ANN is trained by applying the "Levenberg–Marquardt back propagation" (LM) algorithm. LM approximates Newton's method [24].

Over-fitting and under-fitting may occur when applying the ANN model. To mitigate the over-fitting effect, an early stopping technique could be applied. In this work, the early stopping technique was used by at random partitioning of the input dataset into three different quantities: training, validation, and test sets with amounts of 70%, 15%, and 15%, respectively. Afterward, the training dataset was firstly applied to the assessment of the network weights and their bias. Then, the calculated errors are used for an adaptation though learning, i.e., the training process is performed. As soon as the calculated error at the validation point started to increase again for a given number of duplications, the training was stopped to allow for suitable corrections. To ensure the performance, the untrained trained test data were provided to the network. Consequently, the determination coefficient (R^2) of the test-data is an appropriate parameter for identifying over-fitting in the network. The transfer-functions used in the hidden and output layers are linear, log-sigmoid, and tan-sigmoid. In our approach, the optimal architecture of the artificial neural network is a network that has the utmost correlation coefficient (R) and the lowest error rates to predict the correct response. Moreover, the Mean Absolute Error (MAE) (Equation (5)) and the Mean Standard Error (MSE) (Equation (4)) were computed to estimate the accuracy of the prediction models.

$$\mathrm{MSE} = \frac{1}{n}\sum_{i=1}^{n}(Xi - Xj)^2 \tag{4}$$

$$\mathrm{MAE} = \frac{\sum_{i=1}^{n}|zi - yi|}{n} \tag{5}$$

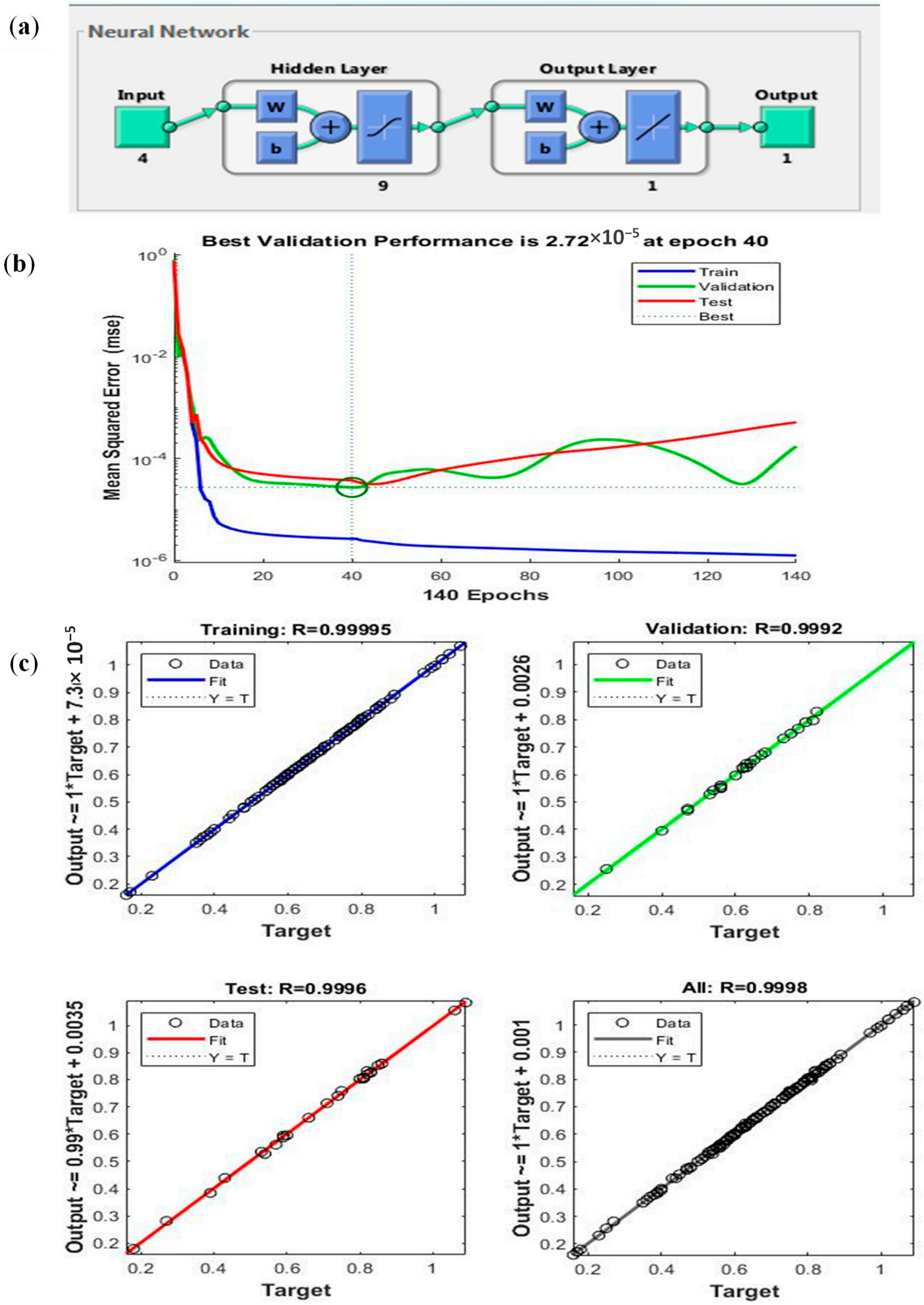

Figure 2. Design (**a**), performance (**b**); Training and validation of variables in Artificial Neural Network model outputs (**b**,**c**).

The Mean Absolute Error defines a linear score. It represents the average of the individual differences. Figure 2b indicates that the values regarding MSE with best validation performance is 2.72×10^{-5} at epoch 40 and the corresponding calculated R value is 0.99995.

The training set value of R^2 = 0.9996 with a validation set R is 0.9992. The validation value from the dataset is 0.9998. The prediction precision of all information sets (training set, validation and testing) is highly adequate and therefore competitive. Analyzing the predicted values in detail, we can observe that the MSE's values were small, which demonstrates that the expected and real values were near to our results. The three coefficients, i.e., the predicted R-squared (0.4475), R-squared (0.9033) and adjusted R-squared (0.7904) values, were in an expected range to one another. The Adeq-Precision measures reflect the signal-to-noise ratio (SNR). In the underlying use application, a SNR greater than 4 is appropriate. In the considered case, the Adeq-precision value appeared to be exactly 14.77 which can be interpreted as an adequate signal. Henceforth, the model showed a promising prediction capability and a high reliability. Nevertheless, the model's components are also specific and crucial. According to the these limitations, some of the RSM's components (AA, B_2, BB, C_2, BC, D_2, and CD) with negligible p value were excluded from the further process.

2.6. Genetic Algorithm (GA) with ANN & RSM Comparison

A GA work is an optimization heuristic. It aims at identifying the optimal solution from the feasible solution area using a fitness (objective) function and its limitation [25,26]. A GA can follow two major directions: focusing on the optimization of single objective function or the optimization of multi-objective functions. An optimization of a single objective function optimizes only one objective and the outcome is a distinctive solution which could be either maximal or minimal. As a basis, a GA considers three primary genetic operations, namely selection, mutation and crossover. To achieve viable results with a GA, the first step is to determine the population size, which may be selected at random according to [27]. Alternatively, expert knowledge can be used if available. Each solution candidate contained in the population is verified by calling the objective function. Those candidate solutions within the population that show the best fitness value are chosen as parents for building the next generation. These parents are then used to create offspring that is added to the new population. To achieve this, the two operators crossover and mutation [28] and applied.

Since we focus on artificial intelligence-based strategies for the modeling and optimization of Pb removal, we utilized a GA for the identification of the optimal conditions for Pb removal. This requires a phytoremediation strategy using the artificial intelligence models defined above (i.e., RSM and ANN). The software used for this purpose is MATLAB 2020a Simulink®. To characterize the fitness functions, the following conditions were determined for the RSM and ANN approaches:

1. Fitness function = 1/4 Min (RSM equation's removal rates)
2. Fitness Function = 1/4 Max (RSM equation's removal rates − 1 × RSM's equation)
3. Fitness function = 1/4 Min (ANN equation's removal rates)
4. Fitness Function = 1/4 Max (ANN equation's removal rates − 1 × RSM's equation)

With the help of the above four equations, we evaluated the best and worst conditions for elimination and removal rate.

3. Results & Discussion

3.1. Tolerance of Bacteria against Pb and Citric Acid

Different bacterial strains (NCCP-1848, NCCP-1857, NCCP-1862, NCCP-1844) pre-isolated by Manzoor et al. [8] were studied for their tolerance against Pb and citric acid concentrations. The results (see Table 2 as well as Figures 1 and 3) indicate that *M. paraoxydans* (NCCP-1848) showed the highest significant dry biomass production and tolerance index towards Pb as well as the citric acid. It was observed that *M. paraoxydans* was resistant up to 800 mg L^{-1} Pb and the citric acid concentrations up to 10 mmol L^{-1}. Furthermore, the results also indicated significantly higher minimum inhibitory concentrations (MIC) in the contradiction of further heavy metals in the sequence of Zn > Ni > Co >Cd, respectively (Table 2). Pb tolerance of *M. paraoxydans* have already been well reported [8,29]. The metabolic profiling of *M. paraoxydans* have shown the production of organic acids (i.e., succinic and acetic acids) that resulted in decreasing the pH values of the medium and thereby improving the fermentation process of coffee beans. Manzoor et al., 2019 [8] and Ribeiro et al., 2020 [30] have also reported on the production of siderophores and indole acetic acid by *M. paraoxydans*, which indicated the ability of bacteria to tolerate and function at low pH conditions that might be caused by citric acid addition. Hence, *M. paraoxydans* was selected for further study.

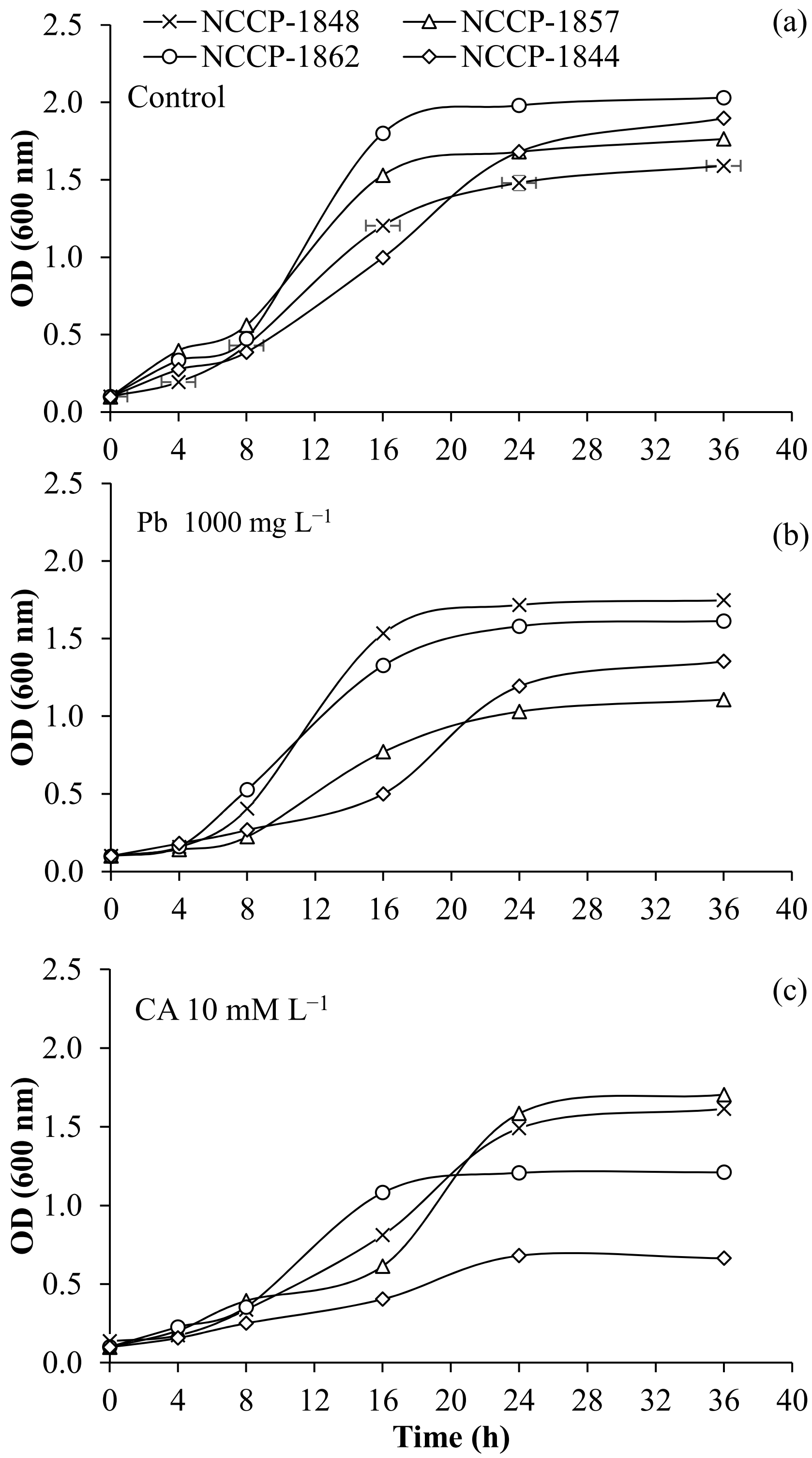

Figure 3. Growth curves of bacterial strains in LB media (**a**); 1000 mg L^{-1} Pb (**b**) and 10 mM citric acid (**c**) at different time intervals.

Table 2. Dry biomass and tolerance index of bacterial strains exposed to different concentrations of citric acid and heavy metals in LB agar and broth, respectively.

Bacterial Strains	Dry Biomass (g) in Pb and CA (1 mM)		Tolerance Index (TI)		Minimum Inhibitory Concentration (mM)					
	Pb	CA	Pb	CA	Pb	Cd	Co	Cu	Ni	Zn
NCCP-1848	0.0	4.0	1.0	1.0	10	0.6	5	8	8	10
NCCP-1857	8.3	12.5	0.9	0.9	5	1	0.5	5	5	10
NCCP-1862	17.9	7.1	0.8	0.9	2	0.5	0.5	2	2	0.5
NCCP-1844	11.5	19.2	0.9	0.8	<0.5	<0.1	1	<0.1	1	2

Tolerance index (TI) = biomass produced with Cd or Pb to that in control. MIC: Minimum inhibitory concentration.

3.2. Effect of Citric Acid Pb and Tolerant Bacteria on Plant Growth and Pb Uptake

The effect of the citric acid and Pb tolerant bacteria on plant growth and Pb removal efficiency was recorded on MS agar plates as well as in pot experiment. The results from the Petri Plate experiment indicated a significant reduction in seed germination (−30%), plant length (−70%) and SVI (−79%) of *P. hortorum* L. when exposed to high Pb concentration (40 mg L^{-1}) (see Figure 1 and Table S3). Upon co-application of *M. paraoxydans* (1.5 OD) and citric acid (10 mmol L^{-1}), the plant growth parameters including germination (1.2-folds), plant length (1.5-folds), SVI (2.2-folds) and plant biomass (1.8-folds) were significantly improved (Table S3 and Figure 4a). This is consistent with the results obtained by Manzoor et al., 2019 [8]), where *M. paraoxydans* individually and in combination with *Mucor* spp. (citric and oxalic acid producing fungi) improved the plant biomass by 1.6- and 2.3-folds, respectively. Besides Pb tolerance (see Table 3) *M. paraoxydans* has also been identified as plant growth promoting rhizobacteria (PGPR) with significant production of IAA (92.3 mg mL^{-1}), ACC deaminase (260 mM aKB mg^{-1} h^{-1}), GA_3 (1.0 mg mL^{-1}), and siderophopre (41.3 units) production [8]. The citric acid has also been reported to increase biomass of *P. hortorum* L. by 18.4% at 1500 mg kg^{-1} soil Pb concentration [3].

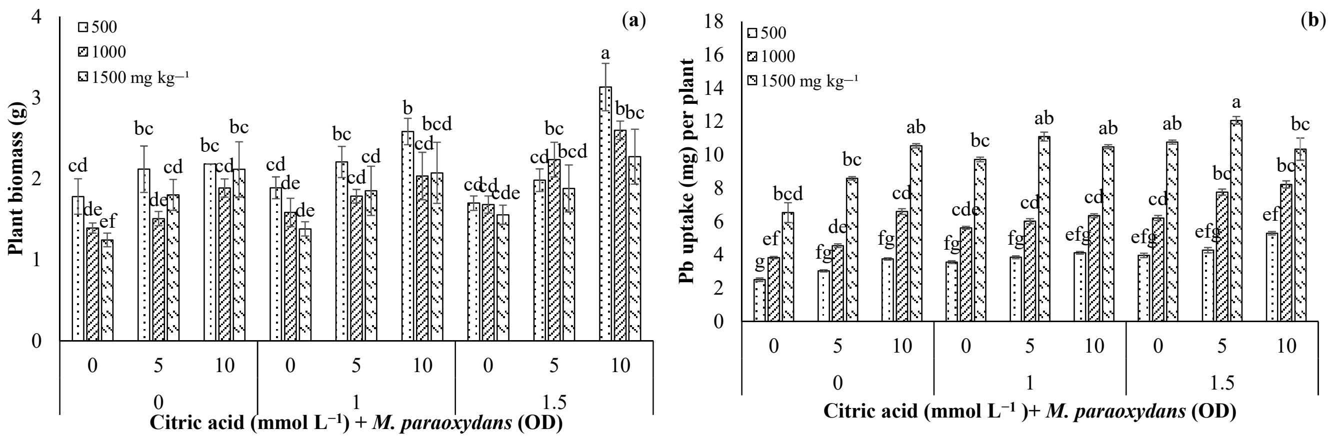

Figure 4. Effect of applying citric acid and *M. paraoxydans* on plant biomass (g) (**a**) and Pb uptake (**b**) in of *P. hortorum* (after 90) exposed to different concentration of soil Pb concentrations (0, 500, 1000 and 1500 mg kg^{-1}). Different letters indicate significant difference at $p < 0.05$.

Similarly, in the pot experiment, the highest significant Pb increase (12.06 mg per plant) was observed upon co-application of *M. paraoxydans* (1.5 OD) and the citric acid (5 mmol L^{-1}) after 90 days at 1500 mg kg^{-1} soil Pb concentration, respectively (Figure 3b). Both, *M. paraoxydans* and citric acid, have been reported to improve the Pb chelation in soil, phytoavailability and the uptake in plant. Manzoor et al., 2019 [8] described that when *M. paraoxydans* was inoculated *P. hortorum* L. had 1.9-folds more Pb compared to un-inoculated control plants at 2000 mg kg^{-1} soil Pb level. Similarly, the Pb uptake in *P. hortorum* L. was observed with 130% using the citric acid (compared to the control plant without the citric acid) at 1500 mg kg^{-1} soil Pb concentration. When compared, the co-application of *M. paraoxydans* and citric acid have a significant ($p < 0.05$) and synergistic effect on the Pb uptake (4.8-folds increase) (Figure 4b), which may be attributed to the improved plant biomass and Pb chelation through lowering soil pH, IAA siderophore production [8], and metal chelation with organic ligands [31].

Table 3. BBD results with independent variable and predicted results of Lead removal.

Run Order	A-Pb Concentration (mg kg^{-1})	B-*M. paraoxydans* (OD)	C-Citric Acid (mgL^{-1})	D-Sampling Days (D)	Y-Lead-Removal (%)	RSM Predicted Value (%)	ANN Predicted Value (%)
1	**500**	**0.00**	**5**	**60**	**58**	57.79	**58.04**
2	**1000**	**1.50**	**10**	**60**	**84**	76.50	**84.10**
3	1000	0.75	0	30	59	60.12	57.79
4	1000	0.75	10	90	62	67.29	61.92
5	500	0.75	0	60	75	69.37	70.89
6	1500	0.75	5	90	70	64.16	71.90
7	**1000**	**0.00**	**10**	**60**	**65**	63.00	**65.32**
8	**1000**	**0.75**	**5**	**60**	**59**	60.33	**59.05**
9	1000	0.00	5	90	48	47.87	47.73
10	1500	1.50	5	60	73	79.62	72.17
11	**1000**	**1.50**	**5**	**90**	**81**	80.87	**81.04**
12	1000	1.50	0	60	83	82.66	82.76
13	**500**	**0.75**	**5**	**30**	**67**	70.50	**67.11**
14	1000	1.50	5	30	80	76.04	79.87
15	1500	0.00	5	60	57	58.12	56.52
16	**1000**	**0.00**	**0**	**60**	**36**	41.16	**36.04**
17	1000	0.75	5	60	62	60.33	59.72
18	1000	0.00	5	30	58	54.04	56.09
19	1000	0.75	0	90	56	57.95	57.80
20	**500**	**0.75**	**5**	**90**	**74**	72.83	**74.00**
21	1500	0.75	0	60	65	62.70	67.74
22	1500	0.75	10	60	70	71.54	65.97
23	1500	0.75	5	30	69	67.83	68.76
24	**500**	**1.50**	**5**	**60**	**86**	91.29	**86.05**
25	1000	0.75	5	60	60	60.33	59.05
26	500	0.75	10	60	78	76.20	77.71
27	1000	0.75	10	30	62	66.45	63.84

3.3. Predicting Pb Removal Using RSM

We conducted experiments to predict the Pb removal with the RSM approach. The results obtained from RSM were fitted to a non-linear quadratic equation with the help of a regression method. The evaluation of the results and the prediction outcomes of the ANN and RSM models are illustrated in Figure 1. After selecting and eliminating the variables with a non-significant factor ($p > 0.05$), Equation (6) was obtained.

$$Y = 86.04 - 1.5 * A + 10 * B + 60.0 * C + 500 * D - 2.0 * A * C - 1.5 * B * C + 36.04 * A^2 \quad (6)$$

In Equation (6), the variables A, B, C, D, and Y represent the Pb concentration of (mg kg^{-1}); the concentration of citric acid (mg L^{-1}); the number of *M. paraoxydans* (OD); the sampling day (day); and the Pb removal rate (%), respectively.

Table 3 illustrates the difference between the experimental results and the predicted results. The observations explain the details of the independent variables with the values of their units according to the BBD approach as responding (−1, 0, 1). It explains the independent variables with a series of Pb concentration, *M. paraoxydans*, citric acid, and sampling days of the variables. Their values show series with lower to higher sequence values, i.e., 500, 1000, and 1500 mg kg^{-1} for the Pb concentration; 0, 0.75, and 1.5 OD for *M. paraoxydans*; 0, 5, and 10 mmol L^{-1} for the citric acid; and 30, 60, and 90 for the sampling days. Table 3 guarantees that the proposed model can predict results with marginal differences. The highest removal rate was observed in Run 2 for the experimental data with 84.10% reliability. For the RSM prediction, the highest removal rate was observed in Run 16 with 86.05%. On the other hand, Run 16 indicates the lowest Pb removal rate with 36.04%. This explains the results in 27 runs with the BBD function, where we used the graph for designing the chart of the run with outcomes. The highest outcome of the ANN is 86.05% with the 500 Pb concentration and the lowest value is 36.04% with the 1000 Pb concentration for the same number of days (i.e., 60 days). The differences among two or more data groups can be significantly examined using the analysis of variance (ANOVA) method. As the name suggests, ANOVA is used in RSM to significantly derive the fitness of the prediction with laboratory findings. Table 4 suggests that the F-value equals to 14.40 and that the p-value is <0.05. This indicates that the second-order regression equation for the response prediction is accurate at the best possible level.

Table 4. ANOVA for response surface quadratic model. (*) indicates interaction among different parameters.

Source	DF	Adj SS	Adj MS	F-Value	p-Value
Model	14	0.318192	0.022728	8.00	<0.000
Linear	4	0.255050	0.063763	22.45	<0.000
A-Pb Cons.	1	0.009633	0.009633	3.39	0.090
B-*M. paraoxydans*	1	0.226875	0.226875	79.90	<0.000
C-Citric	1	0.018408	0.018408	6.48	<0.026
Days	1	0.000133	0.000133	0.05	0.832
Square	**4**	**0.035692**	**0.008923**	**3.14**	**0.055**
A-Pb Cons. * A-Pb Cons.	1	0.032033	0.032033	11.28	0.006
B-*M. paraoxydans* * B-*M. paraoxydans*	1	0.007008	0.007008	2.47	<0.142
C-Citric * C-Citric	1	0.001875	0.001875	0.66	<0.432
D days * D days	1	0.000300	0.000300	0.11	0.751
2-Way Interaction	6	0.027450	0.004575	1.61	<0.227
A-Pb Con * B-*M. paraoxydans*	1	0.003600	0.003600	1.27	<0.282
B-*M. paraoxydans* * C-Citric	1	0.019600	0.019600	6.90	<0.022
C-Citric * D days	1	0.000225	0.000225	0.08	0.783
Error	12	0.034075	0.002840		
Lack-of-Fit	**10**	**0.033608**	**0.003361**	**14.40**	**>0.067 (Non-significant)**
Pure Error	2	0.000467	0.000233		
Total	**26**	**0.352267**			

In Table 4, the larger F-value suggests that the random error is significantly smaller than the variance of the RSM. The achieved F-value is 14.40, which is greater than the reported critical F value (3.14 with an α level of 0.67). This indicates that the BBD model is a good predictor for the experimental data. The proposed model is powerful enough to predict the F-values and other significant parameters.

The estimated t-value, p-value, and regression coefficients for the linear quadratic equation are shown as a summary in Table 4. This also illustrates the variable's interaction effect. When compared to the ANN, it appeared to be 95%, which is a significant level. The p-value can be used to identify the effectiveness of the model. Table 4 explains that the independent variables (i.e., the interaction effect between Pb concentration and time) are all non-significant (p < 0.05). Furthermore, to evaluate the experimental design results, we have used a Pareto analysis. In the equation, (Y) is the percentage influence factor for Pb removal [32]. The Pareto analysis (see Figure S1) shows that *M. paraoxydans* has the maximum P value. This indicates the key effects (A, B, D, E) and further shows that the two-factor interactions (BE) have a significant impact on the mean height at 5%. The normal plot shown in Figure S2a indicate that the residuals fall approximately along a straight line. We may conclude from this that the data show standardized effects with the four factors, A, B, C, and D. The final quadratic polynomial model is presented for getting the optimum

BBD model for Pb removal. This is achieved by removing the insignificant variables that show a non-significant removal rate ($p < 0.05$) (Figure S2). Due to the smallest level of significance (i.e., $p < 0.05$), the model can be statistically considered. The main effects on the four factors are equal to 2.179, and the corresponding Pb removal percentage is at the 5% significance level (Table 4). Based on the graphs in Figures 5 and S3, the RSM and ANN models show the hold values with five factors (Pb concentration, *M. paraoxydans* and Pb extraction, citric acid, and sampling days) with greater elegance. A higher Pb extraction rate of 0.86% was observed in Table 3. A significant decrease in the Pb phytoextraction rate was observed when an increase in the Pb concentration up to 1500 mg kg^{-1} was induced. A negligible but positive effect (at 5 and 10 mmol L^{-1}) on the removal rate was observed while increasing the concentration of the citric acid. The time aspect was also a very effective factor. Figures 1 and 5 also explain the predicted values of the independent variables using the ANN model. The values are close enough to the experimental results.

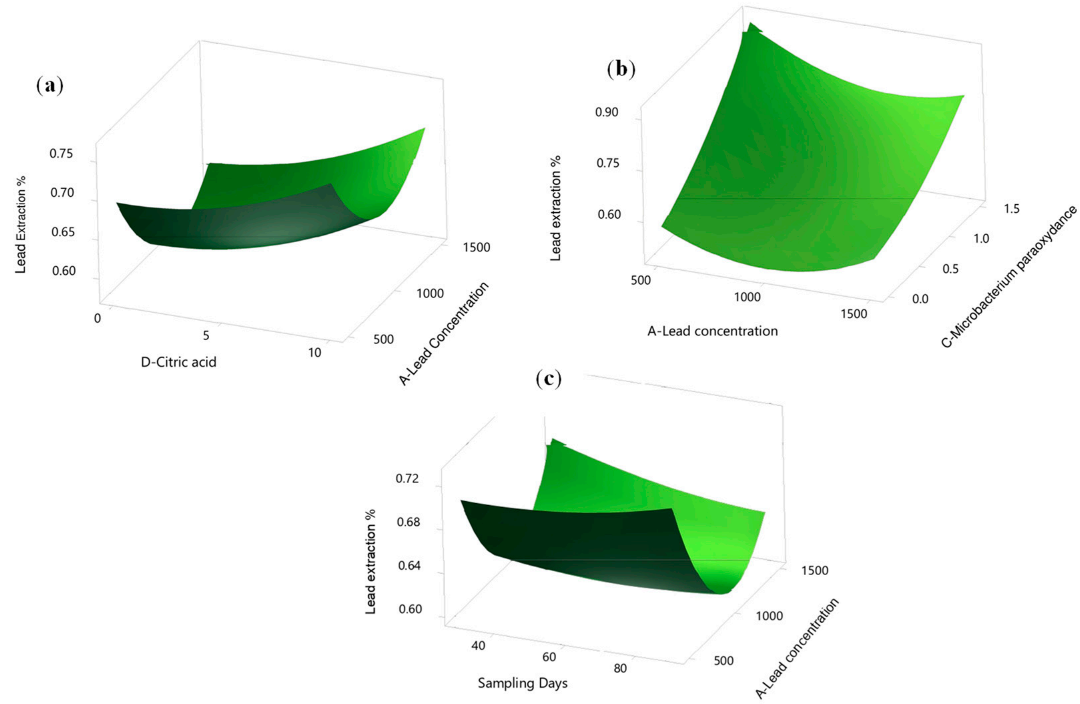

Figure 5. Four factor comparison of ANN with lead concentration vs. hold values of surface plot. Surface plots of lead concentration and citric acid (**a**); lead concentration and *M. paraoxydans* (**b**); and lead concentration and sampling days (**c**).

The residual plot for Y is computed by the division of the residual on an estimated standard deviation (SD). The SD for each residual is calculated separately from the estimated observations. To identify outliers and to evaluate equal variance, the method of Studentized residuals is well-established. Using this approach, the points were found to be linear, as shown in Figure S3a. This demonstrates the normal distribution of errors in our model. Further, non-linear shaped curves identify an asymmetrical error distribution that needs to be modified since the points were linear in our graph. According to the results shown in Figure S2b, the model predicted the expected results with appropriate accuracy. The highest removal rate was observed in Run 2 for the experimental data with 84.10%. Further, the highest removal rate of the RSM prediction was observed in Run 16 with 86.05%. On the other hand, Run 16 indicated the lowest Pb removal rate with 36.04%. Figure S2 essentially conducts a t-test for potential outliers. The plotted graphs do not indicate any noticeable violation of the outliers generated by the model results. The errors identified at all points were in an appropriate range. Figure S2c shows the distance in each run. In the residual case, all fitted values are separated but in a sequence context, we can observe all plotted points. This allows us to detect the dominant points and deals with the frequency against the residual with a histogram graph. The model coefficient estimates the normal probability plot with the residual in Figure S2a. Here, all values are on a single line, which shows a linear coefficient of 1.0, designated as the dominant value. Further, every value that sticks out from the remaining influence is also considered to be dominant. The model is optimally affected by the values that are close to zero or are zero.

3.4. Comparison ANN with Four Factors

The surface plots were constructed as factorial experiments with the help of two factors (*M. paraoxydans* and Pb concentration) based on the BBD method. We used a three replicate plot design for treating and controlling the variables. Significant differences in predicted and laboratory results and means were calculated with ANOVA. The least significant test design (LSD) was performed in Minitab software at $p < 0.05$. The data input into the neural network was given in the form of experimental variables for the estimation of a valid amount of Pb. Figures 1 and 4 demonstrate the training verification data and test dataset for the ANN, which provides the best predictions. Furthermore, statistical performance given in Table 4 was achieved by parameters such as mean (μ), standard deviation (σ), regression coefficient (R^2), and standard error (SE). The value of R in the Levenberg–Marquardt (LM) algorithm is 0 to 1. The LM plot estimates the prospect of the particular points. In the design of the experiment covering the influence, this algorithm finds the values of MSE and MAE with test data of R and the best R's for all datasets. Further it identifies the lowest dataset for the MSE and MAE (Table 5).

Table 5. Training algorithms comparison.

Algorithms	R (Total Value)	R (Test Value)	MSE	MAE
Levenberg–Marquardt LM	0.963	0.998	0.00017	0.0111
Quasi Newton	0.941	0.938	0.00093	0.0310
Scaled Conjugate Gradient	0.932	0.991	0.00498	0.0564
Gradient Descent	0.391	0.490	0.04314	0.180

3.5. Predicting Pb Removing by Phytoremediation with ANN

A 4:4:1 network topology was implemented for the ANN model using several training algorithms to evaluate the best performance. An ANN operates on mathematical nodes that are interconnected with each other (Figure 2). Figure 1 supports the best conditions for the elimination of the max error as well as the worst condition obtained for the Pb removal. The results of the MSE and MAE measure the network performance according to the mean of squared errors (Table 5). The ideal MSE is not "0"—this would be, a model that perfectly predicts our training data values in Figure 1. These findings suggested that in this particular case and other cases of prediction related to removal of containments from the soil, the ANN approach shows promising results compared to the RSM variant in a non-linear regression analyses.

4. Conclusions

In this study, we developed an ANN modeling approach. Compared to the reference solutions, this has several advantages, especially the black box modeling character, the simplicity of the model, and the efficiency. This means that the approach is currently the best choice for modeling complex system behavior, such as waste water management processes. For nearly all experimentations, the ANN has been shown to be a suitable and accurate approach for predictions. In this article, an ANN model was developed using experimental data from the lab. Therefore, a RSM-based BBD approach has been used to study the lead removal from contaminated soil. In a first step, this is achieved by a washing process. We considered two biodegradable chelates (citric acid and *M. paraoxydans*) for the process. The independent variables with their position values were constructed on their respective outcomes of initial single factor tests. All the selected parameters had a positive effect on the process, except for Pb efficiency. The interaction effect between Pb concentration and time are all non-significant ($p < 0.05$). The second-order regression equation for the response prediction is accurate up to the best level. ($R^2 > 0.9033$). This research was completed to identify, depict, and streamline the Pb removal of some Pb-lessening bacteria, which were stemming from various agricultural soil tests. Therefore, the isolation of a new effective strain is significant. As a conclusion, the presented modeling approach uses two different techniques, namely RSM and ANN. According to our sampling tests, the best-fit results were shown by the ANN method in different ways considering the LM algorithm.

Supplementary Materials: The following supporting information can be downloaded at: https://www.mdpi.com/article/10.3390/su151411049/s1. Figure S1: Standardized effects on four factors Pareto chart; Figure S2: Results of RSM predicted model. Normal probability plot (a); histogram plot (b); Residual plots for RSM model output (c and d); Figure S3: RSM response surface plots for lead concentration and sampling days (a); lead concentration and citric acid (b); and lead concentration and *M. paraoxydans* (c); Table S1: Physicochemical characteristics of soil used in experiment; Table S2: Summary of Box–Behnken design; Table S3: Effects of *M. paraoxydans* and citric acid on germination and growth of *P. hortorum* in Petri plates containing 1/2 Murashige and Skoog (MS) agar medium supplemented with different concentrations of Pb (0, 10, 20, 30, and 40 mg L^{-1}).

Author Contributions: M.M. performed the laboratory biochemical analysis and manuscript drafting. U.R.K. planned the experimental design, studied Pb extraction efficiency using artificial neural networks (ANNs) and genetic algorithm (GA) prediction models, and also performed statistical analysis and the interpretation of the data. I.G. and S.G. assisted in the experimental work and preparation of the manuscript. A.S. helped in interpreting and reviewing the manuscript. M.A. and S.T. obtained funding from the PERIDOT international research collaborative program and DFG for the experimental work. All authors have read and agreed to the published version of the manuscript.

Funding: The work was financially supported by DFG Germany. We acknowledge the financial support by the DFG within the funding programme Open Access-Publikationskosten.

Institutional Review Board Statement: Not applicable.

Informed Consent Statement: Not applicable.

Data Availability Statement: All data generated and analyzed in this study are included in this manuscript.

Conflicts of Interest: The authors declare that the work presented in the manuscript is original and is not submitted anywhere for publication. The authors also declare no competing financial interests or personal relationships that could influence the quality of research work presented in this manuscript.

Nomenclature

ANN	Artificial Neural Network
RSM	Response Surface Methodology
GA	Genetic Algorithm
LMA	Levenberg–Marquardt Algorithm
BBD	Box–Behnken design
Pb	Lead
FFBPNN	Feed-Forward Back-Propagation Neural Network
MAE	Mean Absolute Error
CA	Citric Acid
LB	Luria–Bertani
Cu	Copper
Zn	Zinc
Co	Cobalt
Ni	Nickel
pH	Potential of Hydrogen
n	Number of Inputs

i	Increment Variable
μ	Mean
σ	Standard Deviation
R^2	Regression Coefficient
LSD	Least Significant Test Design
OD	Optical Density
MS	Murashige and Skoog
MIC	Minimum Inhibition Concentrations
M. paraoxydance	*Microbacterium paraoxydance*

References

1. Abbassi, F.; Ahmad, F.; Gulzar, S.; Belhadj, T.; Karrech, A.; Choi, H.S. Design of T-shaped tube hydroforming using finite element and artificial neural network modeling. *J. Mech. Sci. Technol.* **2020**, *34*, 1129–1138. [CrossRef]
2. Abbassi, F.; Karrech, A.; Islam, M.S.; Seibi, A.C. Poromechanics of Fractured/Faulted Reservoirs During Fluid Injection Based on Continuum Damage Modeling and Machine Learning. *Nat. Resour. Res.* **2023**, *32*, 413–430. [CrossRef]
3. Albatrni, H.; Qiblawey, H.; Almomani, F.; Adham, S.; Khraisheh, M. Polymeric adsorbents for oil removal from water. *Chemosphere* **2019**, *233*, 809–817. [CrossRef]
4. Antony, J. Multi-response optimization in industrial experiments using taguchi's quality loss function and principal component analysis. *Qual. Reliab. Eng. Int.* **2000**, *16*, 3–8. [CrossRef]
5. ATSDR. *Toxicological Profile for Lead*; Agency for Toxic Substances and Disease Registry: Atlanta, GA, USA, 2007.
6. Gadekar, M.R.; Ahammed, M.M. Modelling dye removal by adsorption onto water treatment residuals using combined response surface methodology-artificial neural network approach. *J. Environ. Manag.* **2019**, *231*, 241–248. [CrossRef]
7. Gul, I.; Manzoor, M.; Hashim, N.; Shah, G.M.; Waani, S.P.T.; Shahid, M.; Arshad, M. Challenges in microbially and chelate-assisted phytoextraction of cadmium and lead—A review. *Environ. Pollut.* **2021**, *287*, 117667. [CrossRef]
8. Gul, I.; Manzoor, M.; Hashmi, I.; Bhatti, M.F.; Kallerhoff, J.; Arshad, M. Plant uptake and leaching potential upon application of amendments in soils spiked with heavy metals (Cd and Pb). *J. Environ. Manag.* **2019**, *249*, 109408. [CrossRef] [PubMed]
9. Gul, I.; Manzoor, M.; Kallerhoff, J.; Arshad, M. Enhanced phytoremediation of lead by soil applied organic and inorganic amendments: Pb phytoavailability, accumulation and metal recovery. *Chemosphere* **2020**, *258*, 127405. [CrossRef]
10. Hassan, S.U.; Haddawy, P.; Zhu, J. A bibliometric study of the world's research activity in sustainable development and its sub-areas using scientific literature. *Scientometrics* **2014**, *99*, 549–579. [CrossRef]
11. Karri, R.R.; Sahu, J. Modeling and optimization by particle swarm embedded neural network for adsorption of zinc (II) by palm kernel shell based activated carbon from aqueous environment. *J. Environ. Manag.* **2018**, *206*, 178–191. [CrossRef]
12. Kumar, V.; Singh, J.; Kumar, P. Heavy metal uptake by water lettuce (*Pistia stratiotes* L.) from paper mill effluent (PME): Experimental and prediction modeling studies. *Environ. Sci. Pollut. Res.* **2019**, *26*, 14400–14413. [CrossRef] [PubMed]
13. Learman, D.R.; Ahmad, Z.; Brookshier, A.; Henson, M.W.; Hewitt, V.; Lis, A.; Kourtev, P.S. Comparative genomics of 16 *Microbacterium* spp. that tolerate multiple heavy metals and antibiotics. *PeerJ* **2019**, *6*, e6258. [CrossRef] [PubMed]
14. Linares-Rodrigue, A.; Ruiz-Arias, J.A.; Pozo-Vazquez, D.; Tovar-Pescador, J. An artificial neural network ensemble model for estimating global solar radiation from Meteosat satellite images. *Energy* **2013**, *61*, 636–645. [CrossRef]
15. Lu, Y.; Luo, D.; Lai, A.; Liu, G.; Liu, L.; Long, J.; Zhang, H.; Chen, Y. Leaching characteristics of EDTA-enhanced phytoextraction of Cd and Pb by *Zea mays* L. in different particle-size fractions of soil aggregates exposed to artificial rain. *Environ. Sci. Pollut. Res.* **2017**, *24*, 1845–1853. [CrossRef]
16. Manzoor, M.; Gul, I.; Ahmed, I.; Zeeshan, M.; Hashmi, I.; Amin, B.A.Z.; Kallerhoff, J.; Arshad, M. Metal tolerant bacteria enhanced phytoextraction of lead by two accumulator ornamental species. *Chemosphere* **2019**, *227*, 561–569. [CrossRef]
17. Manzoor, M.; Gul, I.; Manzoor, A.; Kallerhoff, J.; Arshad, M. Optimization of integrated phytoremediation system (IPS) for enhanced lead removal and restoration of soil microbial activities. *Chemosphere* **2021**, *277*, 130243. [CrossRef] [PubMed]
18. Manzoor, M.; Gul, I.; Silvestre, J.; Kallerhoff, J.; Arshad, M. Screening of indigenous ornamental species from different plant families for Pb accumulation potential exposed to metal gradient in spiked soils. *Soil Sediment Contam.* **2018**, *27*, 439–453. [CrossRef]
19. Zhao, W.; Guo, Y.; Lu, S.; Yan, P.; Sui, Q. Recent advances in pharmaceuticals and personal care products in the surface water and sediments in china. *Front. Environ. Sci. Eng.* **2016**, *10*, 2. [CrossRef]
20. McLaughlin, M.J. *Ageing of Metals in Soils Changes Bioavailability*; International Council on Metals and the Environment: London, UK, 2001.
21. Miao, D.; Young, S.L.; Golden, C.D. A meta-analysis of pica and micronutrient status. *Am. J. Hum. Biol.* **2015**, *27*, 84–93. [CrossRef] [PubMed]
22. Mohammadi, F.; Samaei, M.R.; Azhdarpoor, A.; Teiri, H.; Badeenezhad, A.; Rostami, S. Modelling and optimizing pyrene removal from the soil by phytoremediation using response surface methodology, artificial neural networks, and genetic algorithm. *Chemosphere* **2019**, *237*, 124486. [CrossRef] [PubMed]
23. Moore, F.; Sheykhi, V.; Salari, M.; Bagheri, A. Soil quality assessment using GIS-based chemometric approach and pollution indices: Nakhlak mining district, central Iran. *Environ. Monit. Assess.* **2016**, *188*, 214. [CrossRef] [PubMed]

24. Ribeiro, L.S.; Miguel, M.G.D.C.P.; Martinez, S.J.; Bressani, A.P.P.; Evangelista, S.R.; Batista, C.F.S.; Schwan, R.F. The use of mesophilic and lactic acid bacteria strains as starter cultures for improvement of coffee beans wet fermentation. *World J. Microbiol. Biotechnol.* **2020**, *36*, 1–15. [CrossRef] [PubMed]
25. Sanusi, S.N.A.; Halmi, M.I.E.; Abdullah, S.R.S.; Hassan, H.A.; Hamzah, F.M.; Idris, M. Comparative process optimization of pilot scale total petroleum hydrocarbon (TPH) degradation by *Paspalum scrobiculatum* L. hack using response surface methodology (RSM) and artificial neural networks (ANNs). *Ecol. Eng.* **2016**, *97*, 524–534. [CrossRef]
26. Sutherland, C.; Marcano, A.; Chittoo, B. Artificial neural network-genetic algorithm prediction of heavy metal removal using a novel plant-based biosorbent banana floret: Kinetic, equilibrium, thermodynamics and desorption studies. In *Desalination and Water Treatment*; IntechOpen: London, UK, 2018; pp. 385–411.
27. WHO Lead Poisoning and Health, World Health Organization, 2017. Available online: https://www.who.int/en/news-room/fact-sheets/detail/leadpoisoning-and-health (accessed on 17 August 2022).
28. Witek-Krowiak, A.; Chojnacka, K.; Podstawczyk, D.; Dawiec, A.; Pokomeda, K. Application of response surface methodology and artificial neural network methods in modelling and optimization of biosorption process. *Bioresour. Technol.* **2014**, *160*, 150–160. [CrossRef]
29. Xia, L.; Ma, Z.; Kokogiannakis, G.; Wang, S.; Gong, X. A model-based optimal control strategy for ground source heat pump systems with integrated solar photovoltaic thermal collectors. *Appl. Energy* **2018**, *228*, 1399–1412. [CrossRef]
30. Xia, L.; Ma, Z.; Kokogiannakis, G.; Wang, Z.; Wang, S. A model-based design optimization strategy for ground source heat pump systems with integrated photovoltaic thermal collectors. *Appl. Energy* **2018**, *214*, 178–190. [CrossRef]
31. Zhang, Z.; Sarkar, D.; Levy, F.; Datta, R. Chemically Catalyzed Phytoextraction for Sustainable Cleanup of Soil Lead Contamination in a Community Garden in Jersey City, New Jersey. *Sustainability* **2023**, *15*, 7492. [CrossRef]
32. Zhang, X.; Zhong, B.; Shafi, M.; Guo, J.; Liu, C.; Guo, H.; Peng, D.; Wang, Y.; Liu, D. Effect of EDTA and citric acid on absorption of heavy metals and growth of moso bamboo. *Environ. Sci. Pollut. Res.* **2018**, *25*, 18846–18852. [CrossRef]